Proceedings of the 2014 IEEE/SICE International Symposium on System Integration, Chuo University, Tokyo, Japan, December 13-15, 2014

Terrain Traversability Analysis Using Multi-Sensor Data Correlation by a Mobile Robot

Mohammed Abdessamad Bekhti, Yuichi Kobayashi and Kazuki Matsumura

Abstract— **A key feature for an autonomous mobile robot navigating in off-road unknown areas is environment sensing. Extraction of meaningful information from sensor data allows a good characterization of the near to far terrains, and thus, the ability for the vehicle to achieve its tasks with easiness. We present an image feature extraction scheme to predict mobile platform motion information. For a sequence of run, several images of terrains and vibrations endured by the mobile robot are acquired using a camera and an acceleration sensor. Texture information extracted by the Segmentation-based Fractal Texture Analysis descriptor (SFTA) was used to find correlations with acceleration features quantified using different time analysis parameters. Experimental results showed that texture information is a good candidate to predict running information.**

I. INTRODUCTION

During the last decades, engineers have focused on improvement of off-road navigation abilities of autonomous mobile robots, thus a number of research investigations regarding terrain traversability assessment have been conducted [1]. Unmanned ground vehicles (UGVs) are often designed to conduct missions at remote locations in rough environmental scenarios [2]. Moreover due to terrains' variety, soil types, geometry and appearances, it is not a convenient task to map each environment accurately in advance to ensure success of undertaken operations. Therefore autonomous mobile robots are required to run successfully in unmapped terrain without prior knowledge [3].

To move safely and autonomously in such scenarios, planetary rovers have to sense the terrain in order to reduce and/or avoid scenarios that may jeopardize health, stability of the vehicle, or obstruct the mobile robot from pursuing its targeted operation [4]. In some cases, the robot weight causes terrain deformation, which impacts its behavior and configuration [5]. Terrain feature knowledge can be used to correct trajectory deviations by applying framework such as slip compensation [6], or traction control [7].

Some terrain assessment methods rely exclusively on geometric analysis. 3D points cloud acquired by a range sensor are processed to localize and quantify geometric features and threats within a local Digital Elevation Map (DEM). Then, the DEM is discretised, each cell will be tested for menace. The threats are usually evaluated based on parameters like the slope, roughness and height, that could result in excessive tilt, roughness or step obstacle [8].

Since geometric information may not be enough to guide a mobile robot in areas where different types of terrain may be encountered, as introduced in [9], a more preventive scheme for long rage data was desired. 2D Images can furnish worthy information to complete geometric analysis of a scene as presented in [10], where a method for self-supervised classification of terrain based on geometrical and visual data was proposed. Selected visual information are HSV color represented as a four dimensional vector and wavelet-based texture information. features are then fused through a naive Bayes classifier. Visual appearance methods were introduced for terrain geometric features evaluation.

Haward *et al*. [11] used 2D techniques to obtain terrain navigability factors such as obstacles, roughness, the horizon line and discontinuities. To do so, they used an Artificial Neaural Network (ANN) to map correlated stereo image points of rocks on the horizon line and terrain slope. Four input nodes are required for the ANN corresponding to the pixel locations of the correlated points in the two images, and its output is the terrain slope.

Recent research activities proved that by learning from exteroceptive and proprioceptive data, vehicle's attitude towards future terrain can be predicted [12]. An approach based on learning from features was introduced in [13]. Color information of terrain was used for predicting interaction between the robot and the terrain through a classification scheme. The mobile platform learns terrain assessment from interaction with various type of terrain during training stage, and the exteroceptive information was fused with the relevant Rover Terrain Interaction (RTI) parameters to construct an inference model. It proved to be effective for RTI features like vibration and slip.

However, not only color but texture information can allow better prediction. Texture information can be expressed by a much higher-dimensional vector, and thus provides richer information on the terrain, but a simple classification scheme is not sufficient to effectively utilize its information. In this study, we introduce a method of extracting correlation between exteroceptive and proprioceptive data. Exteroceptive information is based on texture information obtained by Segmentation-based Fractal Texture Analysis (SFTA) [14] of terrain images. As Proprioceptive data, vertical acceleration representative of vibrations endured by the mobile platform while running is considered in this paper. The target set for this robot system is to analyze terrain navigability by predicting from terrain images motion information that will

Mohammed Abdessamad Bekhti is with the Graduate School of Science and Technology, Department of Information Science and Technology, Shizuoka University, Japan bekhti.m.a@gmail.com

Yuichi Kobayashi and Kazuki Matsumura are with the Graduate School of Engineering, Department of Mechanical Engineering, Shizuoka University, Japan tykobay@ipc.shizuoka.ac.jp, matsumura.kazuki.14@shizuoka.ac.jp

978-1-4799-6943-2/14/$31.00 ©2014 IEEE

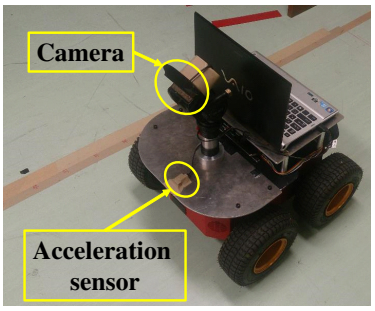

Fig. 1: Pioneer 3AT, equipped with an optical and an acceleration sensor.

help understand robot behavior, and enable a safe run for the mobile robot.

II. Problem Definition

Pioneer 3AT, our experiment platform, is a four wheeled mobile robot equipped with a camera and an acceleration sensor as shown in Fig. 1. The target set in this study is to highlight whether terrain images and mobile robot running data are correlated, *i.e.* a correspondence that translates image features into motion features. If so, the result of data analysis can be employed to analyze terrain traversability beforehand by predicting from terrain images motion information that will help to understand robot behavior and enable a safe run for the mobile robot.

III. Analysis of Correlation Between Motion and Image Features

Overview of the proposed scheme to highlight correlation between image and motion information is shown in Fig. 2. The Region of Interest (ROI) is determined for image feature extraction. As image feature, texture information extracted by Segmentation-based Fractal Texture Analysis (SFTA) will be retained in this study. Regarding extraction of motion features, different time analysis parameters will be considered to describe the motion of the robot. Data matching is carried on to correspond each motion feature data with the generating image features. Data analysis is performed to describe correlation between the set of data. In this study, Canonical Correlation Analysis Analysis (CCA) is used.

A. Region of interest definition

From every terrain image sample, the part of an image corresponding to a short range distance will be considered for image feature extraction. In this section, the camera model is briefly introduced and how it is used to achieve region of interest extraction. Refer to [16] for further details. As shown in Fig. 3, consider a camera with an optical center O_c and an associated camera frame $\{O_c,x_c,y_c,z_c\}$. The relationship between a point in the world reference frame represented by $P \in \mathbb{R}^4$ and its projection $p \in \mathbb{R}^3$ (both containing one as the last element) onto the image plane is given by the following:

$$p = \mathbf{K}[\mathbf{R}|t]P, \tag{1}$$

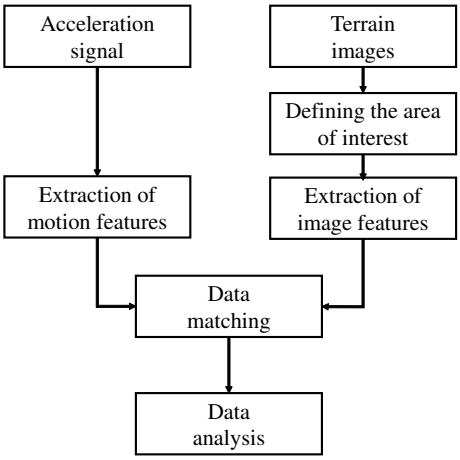

Fig. 2: Overview for data feature extraction and analysis.

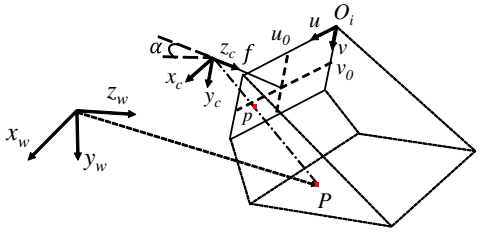

Fig. 3: Projection of the 3D point P in world space onto the image space.

where $[\mathbf{R}|t] \in \mathbb{R}^{4\times4}$ is the rotation and translation transformation, known as extrinsic parameters, that maps homogeneous coordinates from world frame to camera frame. $\mathbf{K} \in \mathbb{R}^{4\times3}$ is the camera parameter matrix expressed as

$$\mathbf{K} = \begin{bmatrix} fs_x & fs_\theta & u_0 & 0 \\ 0 & fs_y & v_0 & 0 \\ 0 & 0 & 1 & 1 \end{bmatrix}, \tag{2}$$

where the pair (u_0,v_0) is the principal point position in pixels, f represents the focal length corresponding to the distance of the image plane from the center of projection, s_x and s_y are the number of pixels per unit distance in image plane in horizontal and vertical directions, respectively. s_θ is equivalent to $\cos\theta$ of the angle formed by image x and y axes.

The above mentioned framework will be used in order to extract the ROI which constitutes the regions of the terrains on which robot wheels are stepping. Using robot dimensions, these regions will be determined on the terrain images. Two parameters are needed, the robot wheels base L and the wheels width W. As shown in Fig. 4, both camera and world reference frame origins, both of which are vertically aligned, are positioned in a away to divide the platform into two symmetric parts virtually. Any point laying on the ground can be projected onto the image plane. Let the world reference frame be defined by $\{O_w,x_w,y_w,z_w\}$, where O_w denotes its origin. We are interested in projecting the following points to determine the inner and outer band of the region of terrain on which the mobile platform is traversing. Knowing that all the points constituting a bound lay on the same line, only the depth components *i.e.* according to the w_z-axis will change. For both left and right sides, these points are given

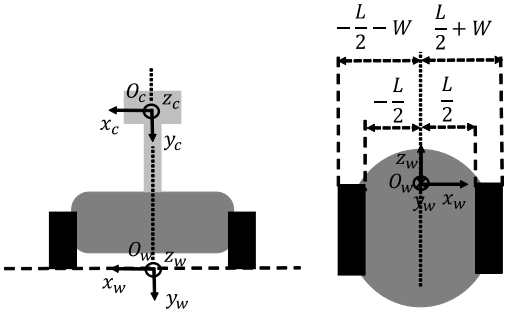

Fig. 4: Mobile robot carrying a camera and layout of both world and camera reference frames.

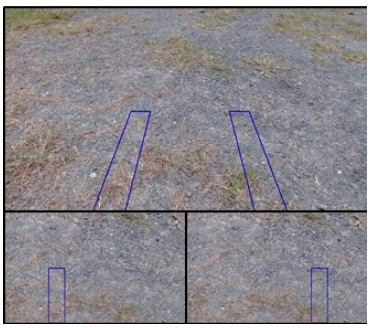

Fig. 5: Region of interest extraction based on the robot dimensions.

as follows:

$$\begin{cases} P_{\text{ro}} = [\frac{L}{2} + W, \quad 0, \quad z_w] \\ P_{\text{ri}} = [\frac{L}{2}, \quad 0, \quad z_w] \\ P_{\text{lo}} = [-\frac{L}{2} - W, \quad 0, \quad z_w] \\ P_{\text{li}} = [-\frac{L}{2}, \quad 0, \quad z_w] \end{cases}, \tag{3}$$

where P_{ro}, P_{ri} denote the points laying on the right outer and inner bounds respectively and P_{lo}, P_{li} the left outer and inner bounds. By changing the component z_w, all the points can be mapped on the image. Results of this operation are shown in Fig. 5. Once the right and left ROIs are extracted, a perspective wrap transformation is performed to remove the trapezoidal shape introduced the moment of taking a picture.

B. Texture features extraction

Texture feature extraction is done by employing SFTA [14]. The SFTA method can be devised into a set of two parts: as the first part, an input grayscale image is decomposed into a set of binary images. To do so, the Two-Threshold Binary Decomposition (TTBD) introduced in [14] is employed. As the second part, each binary image is used to quantify the fractal dimension from its region boundaries, as well as regions mean gray level and size. TTBD computes a set of thresholds T, which is acheived by the Multi-level Otsu algorithm [15]. The multi-level Otsu algorithm aims to find the threshold that maximizes the input image between-class variance. Then, repeatedly, the process is applied to each image to obtain the number of thresholds n_{t} defined by the user. After that, pairs of contiguous thresholds $T \cup \{n_{\text{l}}\}$ with n_{l} the highest value in the input gray scale image, combined with pairs of thresholds $\{t, n_{\text{t}}\}$ with $t \in T$ are used to obtain a set of binary images as follows:

$$I^b_{x,y} = \begin{cases} 1, & \text{if } t_{\text{l}} < I(x,y) \leq t_{\text{u}} \\ 0, & \text{otherwise} \end{cases}, \tag{4}$$

where $I^b_{x,y}$ denotes the binary image, t_{l} and t_{u} denote the lower and the upper threshold values respectively. Consequently, $2n_{\text{t}}$ binary images will be obtained. The SFTA feture vector include three elements, binary image size, mean gray level, and fractal dimension of the boundaries. $\Delta(x,y)$ represents the border image of the binary image $I^b_{x,y}$, and is evaluated as follows:

$$\Delta(x,y) = \begin{cases} 1, & \text{if } \exists (x',y') \in N_{x,y} \\ & \quad s.t.\ I^b_{x',y'} = 0 \wedge I^b_{x,y} = 1 \\ 0, & \text{otherwise} \end{cases},$$

where $N_{x,y}$ is the 8-connexity of a pixel x, y. $\Delta(x,y)$ takes the value one if the pixel at location (x,y) in the related binary image $I^b_{x,y}$ has the value one and having a minimum of one pixel with value zero in its neighborhood. Using the border image, the fractal dimension $D \in \mathbb{R}$ is quantified by the box counting algorithm. The box counting algorithm is defined as follows:

$$D_0(x,y) = \lim_{\varepsilon \to 0} \frac{\log N(\varepsilon)}{\log(\varepsilon^{-1})}, \tag{5}$$

where $N(\varepsilon)$ is the counting of hyper-cubes of length ε that fill the object. By modifying the length of the box ε, one can create a curve of the number $\log \bar{N}(\varepsilon)$ of squares of length ε containing a minimum of one pixel of the object, with respect to $\log(\varepsilon^{-1})$. Using a line fitting method, the fractal dimension D can be calculated as the line's slope. Let $\boldsymbol{x}$ denote an SFTA feature vector. The final dimension of the feature vector depends on the number of desired thresholds n_{t} producing $2n_{\text{t}}$ binary images, since each one of them provides three elements, and thus $\boldsymbol{x} \in \mathbb{R}^{6n_{\text{t}}}$.

C. Extraction of Motion Features

Let $a_k, k = 1, \cdots, K$ be the vertical acceleration signal with time step k and K is the total time step for a sequence of run on a short range distance. In this study, the following time analysis parameters were extracted to describe the motion of the platform: Amplitude distance, Root Mean Square (RMS), Skewness, Kurtosis, and the Crest factor.

1) Amplitude distance: Amplitude distance is the distance between maximum and minimum amplitudes. It is quantified as follows:

$$a_{k_{\text{d}}} = \max_{k=1,\cdots,K} a_k - \max_{k=1,\cdots,K} a_k. \tag{6}$$

2) Root Mean Square: The quadratic mean is an evaluation of the magnitude of a varying signal. In the case of acceleration signal a_k, $a_{k\text{rms}}$ is expressed as follows:

$$a_{k\text{rms}} = \sqrt{\frac{1}{K} \sum_{k=1}^{K} a_k^2}. \tag{7}$$

3) Skewness: Skewness is a measure of the asymmetry of the probability distribution of a real-valued random variable about its mean. It is expressed as follows:

$$a_{k\text{skewness}} = \frac{1}{K\sigma^3}\sum_{k=1}^{K}(a_k - \bar{a})^3, \tag{8}$$

where σ denotes the standard deviation of a_k.

4) Kurtosis: Kurtosis is a measure of the peakedness of the probability distribution of a real-valued random variable.

$$a_{k\text{kurtosis}} = \frac{1}{K\sigma^4}\sum_{i=1}^{K}(a_k - \bar{a})^4. \tag{9}$$

5) Crest factor: Crest factor is a measure of a waveform, such as alternating current or sound, showing the ratio of peak values to the average value. In other words, crest factor indicates how extreme the peaks are in a waveform. Crest factor 1 indicates no peaks, such as direct current. Higher crest factors indicate peaks, for example sound waves tend to have high crest factors.

$$a_{k\text{CF}} = \frac{\max_{k=1,\cdots,K} a_k}{a_{k\text{rms}}} \tag{10}$$

D. Data matching

Before introducing how image and motion features are matched, a brief review of mobile robot motion is introduced. With reference to Fig. 6, the gray circle is the robot and the black rectangle are the wheels. The wheel base *i.e.* how far are the wheels from each other is denoted as L, and the wheels radius is denoted as r representing the size of the wheels. As input information to our system, we have at our disposal v_l and v_r which respectively are the rate at which the left and right wheels turn. The latters are used to describe the robot behavior as follows:

$$\begin{cases} z(t) = \frac{r}{2}(v_\text{l} + v_\text{r})\cos\phi \\ x(t) = \frac{r}{2}(v_\text{l} + v_\text{r})\sin\phi \\ \phi = \frac{r}{L}(v_\text{l} - v_\text{r}) \end{cases}, \tag{11}$$

where x and z constitute the robot position and ϕ its heading or orientation. For our study, both left and right wheels velocities are equal, and thus the robot will move according to the world Z_w-axis.

As mentioned above, only a short range segment of the terrain covered by a single frame will be considered for image feature extraction. Thus, only the relevant part of the acceleration signal generated by running on that proper segment will be focused on for motion feature extraction. During a duration of time, in a simultaneous fashion, acceleration and robot position data are gathered every period on a time scale, *i.e.* the position of the robot can be estimated at any time and how much is the acceleration at the same position. Terrain observations are taken every space interval d_s. Sample terrain images are shown in Fig. 7.

As shown in Fig. 8, at time $t = 0$, the robot is at the origin of the world reference frame. N_image denotes the total number of terrain images gathered during a sequence of a run and d_s denotes the step distance according to the Z_w-axis. Position to take new picture is denoted as $Z_{I_i(x,y)}$ and is expressed as follows:

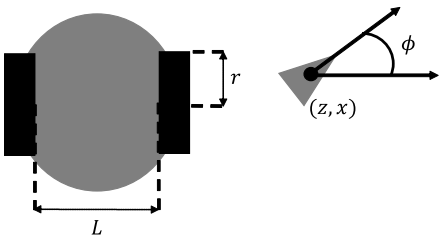

Fig. 6: Differential drive mobile robot.

Fig. 7: Sample terrain observations

$$Z_{I_i(x,y)} = id_s, \quad i = 1, \cdots, N_\text{image}. \tag{12}$$

Due to the camera tilt angle α, terrains will be covered from a certain position expressed as follows:

$$Z_{I_i(x,y)} + Z_\text{BZ}, \quad i = 1, \cdots, N_\text{image}, \tag{13}$$

where Z_BZ is the blind zone not covered by the image. As mentioned above, a short range distance l covered by the images will be retained for image feature extraction. A reason for that is the further a pixel (x, y) is from the camera focus point, the more noise the pixel will be subject to. Thus visual representation of the environment may not be faithful to the real world. Also, only the acceleration signal generated by the distance l will be used for motion feature extrcation.

ROI denoted as A and relevant acceleration signal will be bounded according the Z_w-axis as follows:

$$A_i = [Z_{I_i(x,y)} + Z_\text{BZ}, Z_{I_i(x,y)} + Z_\text{BZ} + l]. \tag{14}$$

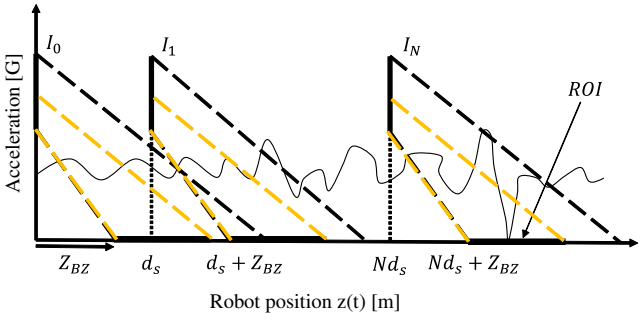

Fig. 8: data acquisition

E. Data analysis using CCA

As mentioned above, our goal is to highlight a potential correspondence between image and acceleration features. If any relationship is established, it will be easy to predict running information of the robot from image features. For this, CCA is used since it allows to compare two groups of quantitative variables to determine if they describe a common phenomenon.

$\boldsymbol{x_i}$, $i = 1, \cdots, N_{\text{image}}$ and y_i, $i = 1, \cdots, N_{\text{image}}$ denote image feature vector and motion feature of the i-th sample image of a terrain respectively. Let N_{terrain} denote the total number of terrain samples and for the j-th terrain sample the data above can be written as follows:

$$\mathbf{X}_j = [\boldsymbol{x}_1 ... \boldsymbol{x}_{N_{\text{image}}}] \in \mathbb{R}^{N_{\text{image}} \times 6n_{\text{t}}}, \quad j = 1, \cdots, N_{\text{terrain}},$$
$$\boldsymbol{y}_j = [y_1 ... y_{N_{\text{image}}}] \in \mathbb{R}^{N_{\text{image}}}, \quad j = 1, \cdots, N_{\text{terrain}}.$$

Finally data matrices needed for correlation analysis are constructed as follows:

$$\mathbf{X} = [\boldsymbol{X}_1 ... \boldsymbol{X}_{N_{\text{terrain}}}] \in \mathbb{R}^{N_{\text{terrain}} N_{\text{image}} \times 6n_{\text{t}}}, \tag{15}$$
$$\mathbf{Y} = [\boldsymbol{y}_1 ... \boldsymbol{y}_{N_{\text{terrain}}}] \in \mathbb{R}^{N_{\text{terrain}} N_{\text{image}}}. \tag{16}$$

Then, CCA is applied to the above matrices and coefficients $\boldsymbol{a} \in \mathbb{R}^{6n_{\text{t}}}$ and $b \in \mathbb{R}$ are computed so as to maximize $\rho(\boldsymbol{a}, b)$, which is expressed as follows:

$$\rho(\boldsymbol{a}, b) = \frac{\boldsymbol{a}^\top \mathbf{S_{XY}} b}{\sqrt{\boldsymbol{a}^\top \mathbf{S_{XX}} \boldsymbol{a}} \sqrt{b \mathbf{S_{YY}} b}}. \tag{17}$$

$\mathbf{S_{XX}} = \frac{1}{N} \tilde{\mathbf{X}}^\top \mathbf{X}$, $\mathbf{S_{YY}} = \frac{1}{N} \tilde{\mathbf{Y}}^\top \mathbf{Y}$, and $\mathbf{S_{XY}} = \frac{1}{N} \tilde{\mathbf{X}}^\top \mathbf{Y}$ are covariance matrices. $\tilde{\mathbf{X}}$ and $\tilde{\mathbf{Y}}$ are as follows:

$$\tilde{\mathbf{X}} = [\boldsymbol{x}_1 - \bar{\boldsymbol{x}} \ \ldots \ \boldsymbol{x}_N - \bar{\boldsymbol{x}}], \quad \bar{\boldsymbol{x}} = \frac{1}{N_{\text{image}} \times N_{\text{terrain}}} \sum_{i=1}^{N} \boldsymbol{x}_i,$$

$$\tilde{\mathbf{Y}} = [y_1 - \bar{y} \ \ldots \ y_N - \bar{y}], \quad \bar{y} = \frac{1}{N_{\text{image}} \times N_{\text{terrain}}} \sum_{i=1}^{N} y_i.$$

IV. Experiment and Results

A. Condition

The proposed scheme was evaluated by running the robot inside university campus. The following parameters settings were used for experiment:

- Wheel base L: 320 [mm],
- Wheel radius wd: 80 [mm],
- Camera height h: 540 [mm],
- Camera tilt angle α: 31[deg],
- Number of thresholds for SFTA n_{t}: 8,
- ROI length l: 500 [mm],
- Blind zone length Z_{BZ} : 400 [mm],
- Number of images per terrain N_{image}: 7,
- Number of sample terrains N_{terrain}: 10,
- Acceleration signal length K: 2,000 samples,
- Acceleration signal sampling period T_s: 10 [ms],
- Step distance for taking images d_s: 500 [mm].

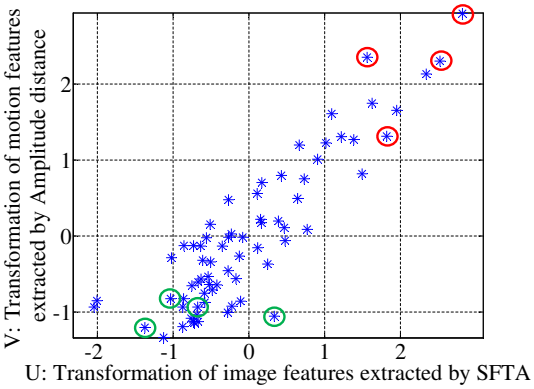

Fig. 9: Result of correlation for right side in the (U, V) space.

B. Results

Results of correlation by computing CCA over all data set are introduced in Table I. High value of correlation coefficients clearly show that texture information extracted by SFTA is highly correlated with motion information.

	Left side	Right side
Amplitude distance	0.8920	0.8908
Root Mean Square	0.7819	0.9166
Kurtosis	0.7804	0.8843
Skewness	0.9011	0.8718
Crest Factor	0.9079	0.8897

TABLE I: Correlation coefficient values.

The aim for data analysis is to describe a certain tendency between image features extracted and relevant motion features.

Red circled points on both Fig. 9 and Fig. 10 indicate that transformed image feature corresponds to high values of transformed motion features. These data points are related to rough terrains shown by Fig. 11. When the mobile platform runs on such rigid terrains, high vibrations or shocks can be witnessed. In fact, amplitude distance for those sample terrains are laying in the range $[1.131, 1.6487]$ [G].

Green circled points on both Fig. 9 and Fig. 10 shows transformed image feature corresponds to low values of transformed motion features. These data points are related to less rough or smooth terrains shown by Fig. 12. When the mobile platform runs on such rigid terrains, low vibrations can be observed. Amplitude distance for those terrains are laying in the range $[0.324, 0.4465]$ [G].

V. Conclusion and Future Work

In this study, we proposed a scheme based on correlation of exteroceptive (terrain observations or images) and proprioceptive (acceleration signals) information to assess terrain maneuverability for mobile robots navigating autonomously in outdoor rigid environment. As image information, texture obtained by SFTA was considered in this study. For motion information, different time signal analysis factors were investigated. The results showed high values for correlation coefficient. Moreover, tendencies with regard to amplitude distance, could be found. High values for transformed motion

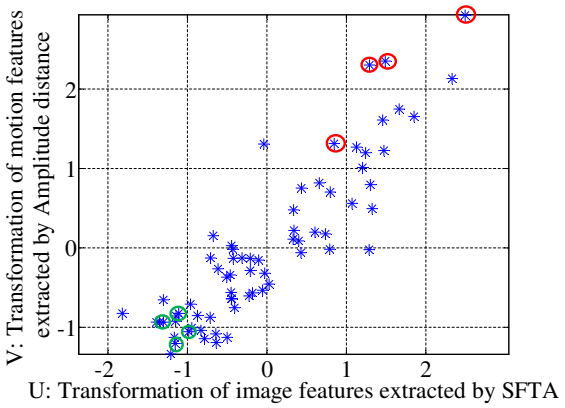

Fig. 10: Result of correlation for left side in the (U, V) space.

Fig. 11: Rigid unstructured terrains.

features translate into rough terrains producing high vibrations or shocks, while low values translate into less rigid or smoother terrains. Based on this trend, terrain traversability comfortableness can be determined where terrains with low values of transformed motion characteristics will be prioritized when navigating. In this study, only the difference of amplitude between the highest and lowest vibrations noticed was considered to describe the roughness of terrain.

As a future work, we propose to apply some prediction to evaluate the performance of our method and performing online process. Also, we plan to assess the repetitiveness of shocks to describe in a better way how rigid a terrain is, and thus a better evaluation of the traversability. Even though good correlation and tendencies were obtained, a one time major vibration can be less harmful to the platform compared to more occurring shocks. The current framework is based on Canonical Correlation Analysis, a linear method

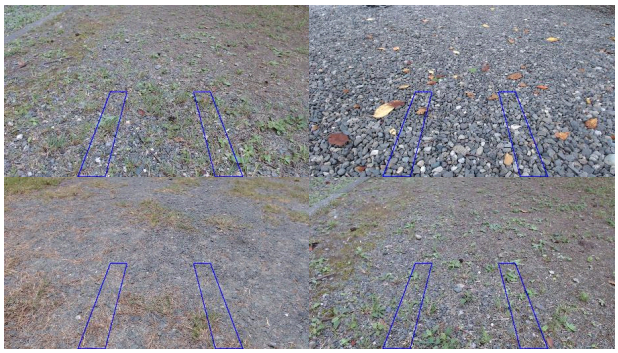

Fig. 12: Less rough terrains.

which happened to be unstable in some cases to find optimal correspondence between image and motion features, this can be seen from the difference of left and right correlation coefficients values in the case of Root Mean Square and Kurtosis. More advanced framework will be investigated in order to strengthen the method. Also, a more variety of terrain will be considered, more precisely artificial grounds made from tiles or asphalt which may furnish rich texture information while actual vibration will be low, the objective is to be able to discriminate terrains type to enable navigability in a wide range of environments.

ACKNOWLEDGEMENT

This research was partly supported by JSPS KAKENHI Grant Number 25330305.

REFERENCES

[1] D. Sancho-Pradel and Y. A Gao, A survey on terrain assessment techniques for autonomous operation of planetary robots, *Journal of the British Interplanetary Society*, vol. 63, 2010, pp. 206-217.

[2] H. Dahlkamp, A. Kaehler, D. Stavens, S. Thrun, and G. Bradski, "Self-supervised Monocular Road Detection in Desert Terrain," *in Robotics: Science and Systems*, Philadelphia, USA, 2006.

[3] A. Stentz and M. Hebert, A complete navigation system for goal acquisition in unknown environments, *Autonomous Robots*, vol. 2, 1995, pp 127-145.

[4] H. Ken, T. Peynot, and S. Sukkarieh, "A near-to-far non-parametric learning approach for estimating traversability in deformable terrain," *in IEEE/RSJ International Conference on Intelligent Robots and Systems*, 2013.

[5] H. Inotsume, M. Sutoh, K. Nagaoka, K. Nagatani, and K. Yoshida, "Evaluation of the Reconfiguration Effects of Planetary Rovers on their Lateral Traversing of Sandy Slopes," *in IEEE International Conference on Robotics and Automation (ICRA)*, 2012.

[6] Daniel M. Helmick, Stergios I. Roumeliotis, Yang Cheng, Daniel S. Clouse, Max Bajracharya and Larry H. Matthies, Slip-compensated path following for planetary exploration rovers, *Advanced Robotics*, vol. 20, 2006, pp. 1257-1280.

[7] K. Yoshida, H. Hamano, and T. Watanabe, "Slip-based Traction Control of a Planetary Rover," *in Experimental Robotics VIII*, vol. 5, Berlin Heidelberg, pp. 644-653, 2003.

[8] M. Maimone, J. Biesiadecki, E. Tunstel, Y. Cheng and C. Leger, *Intelligence for Space Robotics*, TSI Press, 2006.

[9] M. Bajracharya, Benyang Tang, A. Howard, M. Turmon and L. Matthies, "Learning long-range terrain classification for autonomous navigation," *in IEEE International Conference on Robotics and Automation (ICRA)*, Pasadena, CA, pp. 4018-4024, 2008.

[10] C.A Brooks and K.D Iagnemma, "Self-Supervised Classification for Planetary Rover Terrain Sensing," *in IEEE Aerospace Conference*, pp. 1-9, 2007.

[11] A. Howard and H. Seraji, Vision-based terrain characterization and traversability assessment, *Journal of Robotic Systems*, vol. 18, 2001, pp. 577-587.

[12] A. Howard, M. Turmon, L. Matthies, B. Tang, A. Angelova, and E. Mjolsness, Towards learned traversability for robot navigation: From underfoot to the far field, *Journal of Field Robotics*, vol. 23, no. 11-12, 2006, pp. 1005-1017.

[13] A. Krebs, C. Pradalier, and R. Siegwart, Adaptive rover behaviour based on online empirical evaluation: Rover-terrain interaction and near-to-far learning, *Journal of Field Robotics*, vol. 27, no. 2, 2010, pp. 158-180.

[14] A. F. Costa, G. Humpire-Mamani, and A. J. M. Traina, "An Efficient Algorithm for Fractal Analysis of Textures," *in Graphics, Patterns and Images (SIBGRAPI), 2012 25th SIBGRAPI Conference on*, pp. 39-46, 2012.

[15] P. Liao, T. Chen, and P. Chung, A Fast Algorithm for Multilevel Thresholding, *Journal of Information Science and Engineering*, vol. 17, no. 5, 2001, pp. 713-727.

[16] R. Hartley and A. Zisserman, *Multiple View Geometry in Computer Vision*, Cambridge Univ. Press, Cambridge, UK, 2000.